

DETECTION OF AGGLOMERATION IN A FLUIDIZED BED USING STRUCTURE  
FUNCTION

by

Samy Timalsina

Submitted in Partial Fulfillment of the Requirements

for the Degree of

Master of Science

in the

Electrical and Computer Engineering

Program

YOUNGSTOWN STATE UNIVERSITY

August, 2018

DETECTION OF AGGLOMERATION IN A FLUIDIZED BED USING STRUCTURE  
FUNCTION

Samy Timalsina

I hereby release this thesis to the public. I understand that this thesis will be made available from the OhioLINK ETD Center and the Maag Library Circulation Desk for public access. I also authorize the University or other individuals to make copies of this thesis as needed for scholarly research.

Signature:

---

*Samy Timalsina*, Student

Date

Approvals:

---

*Dr. Faramarz D. Mossayebi*, Thesis Advisor

Date

---

*Thomas J. Flynn*, Committee Member

Date

---

*Dr. Jozsi Z. Jalics*, Committee Member

Date

---

Dr. Salvatore A. Sanders, Dean of Graduate Studies

Date

## ABSTRACT

Agglomeration is one of the major problems in fluidized bed processes which affects the uniform distribution of heat and may lead to defluidization and costly shutdown of the whole installation. Detecting the onset of agglomeration before it happens makes it possible to operate the plant more efficiently. The objective is to detect the onset of such undesired behavior with a minimum number of sensors. This research focuses on detecting agglomeration using a nonlinear statistic called the structure function. Because of the simplicity of this technique given its use of a single pressure sensor time series, it is also suitable for on-line detection. The single sensor data exhibits a Gaussian distribution when the bed is well fluidized and changes its dynamics during agglomeration often leading to a periodic pattern in the fluidized bed differential pressure measurement fluctuations. Structure function with orders 2 and 3 are suitably applied to the filtered data of the differential pressure drop from the fluidized bed. Before applying the structure function, the sensitivity analysis of structure function with respect to time lag and window size is performed and optimum values of these two parameters are chosen. Both the second and the third order structure function give the same information about the onset of agglomeration.

## ACKNOWLEDGEMENTS

I would like to take this opportunity to thank Dr. Faramarz D. Mossayebi for providing me this thesis topic and giving me tremendous insights on how to approach a challenging problem. Special thanks goes to Thomas J. Flynn, Timmothy A Fuller, and Prasana Seshadri, from the B&W research lab at Barberton, Ohio, for providing the experimental data and background information. I would also like to thank the faculty of the Department of Electrical and Computer Engineering and the Department of Mathematics at Youngstown State University specifically Dr. Jozsi Z. Jalics. Through their combined efforts, I have gained valuable knowledge and skills that have guided me through my education and this thesis work.

I would also like to thank my family and friends. Without their motivation, I would not have been able to complete the endeavor.

## TABLE OF CONTENTS

CHAPTER I INTRODUCTION .....	1
1.1 Motivation and Background .....	1
1.2 Purpose.....	2
1.3 Goal.....	3
1.4 Objectives .....	3
1.5 Organization.....	3
CHAPTER II BACKGROUND INFORMATION .....	5
2.1 Fluidized bed combustion.....	5
2.2 The fluidized-bed process.....	5
2.3 Agglomeration .....	8
2.4 Structure function and its application to non-linear time series data.....	8
CHAPTER III B&W EXPERIMENTAL SET-UP .....	13
3.1 Experimental.....	13
3.2 Pressure Measurement .....	13
3.3 Data Collection .....	15
CHAPTER IV RESULTS AND DISCUSSIONS.....	17
4.1 Application of Structure Function to BFB Differential Pressure Time Series .....	17
4.2 Sensitivity Analysis of Structure Function with respect to Time-lag.....	20
4.3 Sensitivity Analysis of Structure function with respect to window size .....	25
4.4 Structure function applied to BFB data .....	31
CHAPTER V CONCLUSION .....	38
REFERENCES .....	40

APPENDICES .....	42
1. PROGRAM 1 GENERAL SECOND ORDER STRUCTURE FUNCTION .....	43
2. PROGRAM 2 FILTERING OF RAW DATA.....	44
3. PROGRAM 3 NORMALIZATION OF FILTERED DATA .....	45
4. PROGRAM 4 OPTIMUM TIME LAG SELECTION .....	46
5. PROGRAM 5 OPTIMUM TIME LAG VS. SF PLOT .....	47
6. PROGRAM 6 OPTIMUM WINDOW SIZE SELECTION .....	48
7. PROGRAM 7 WINDOW SIZE VS. SF PLOT .....	49
8. PROGRAM 8 SF TREND WITH ERROR BAR.....	50

## LIST OF FIGURES

Figure 2-1 Different state of fluidized bed .....	7
Figure 2-2 Effect of velocity on bed pressure drop (adapted from B&W, Steam) .....	7
Figure 3-1 Fluidized-bed experimental set-up .....	15
Figure 4-1 time-series plot of differential pressure fluctuations .....	18
Figure 4-2 Filtered with butter worth filter and normalized around central mean .....	19
Figure 4-3 Average 2 <sup>nd</sup> order SF vs. time lag for Chunk 85, 86, 87, 88 .....	21
Figure 4-4 Average 2 <sup>nd</sup> order Sf Vs. time lag for chunk 100, 101, 102, 103 .....	22
Figure 4-5 Average 2 <sup>nd</sup> order SF vs. time lag of chunk 116, 117, 118, 119 .....	22
Figure 4-6 Average 2 <sup>nd</sup> order SF vs. time lag of chunk 127, 128, 129, 130, 131, 132, 133 .....	23
Figure 4-7 Average 2 <sup>nd</sup> order SF vs. time lag of chunk 228, 229, 230 .....	23
Figure 4-8 Average 3 <sup>rd</sup> Order SF vs. time lag of chunk 85, 86, 87, 88 .....	24
Figure 4-9 Average 3 <sup>rd</sup> order SF vs. time lag of chunk 126 through 132 .....	24
Figure 4-10 Average 3 <sup>rd</sup> order SF vs. time lag of chunk 180, 181, and 182 .....	25
Figure 4-11 Average 3 <sup>rd</sup> order SF vs. time lag of chunk 226 through 230 .....	25
Figure 4-12 Avg. Second Order SF vs Window size of chunk 82 .....	26
Figure 4-13 Avg. Second Order SF vs Window size of chunk 110 .....	27
Figure 4-14 Avg. Second Order SF vs Window size of chunk 132 .....	27
Figure 4-15 Avg. Second Order SF vs. Window size of chunk 215 .....	28
Figure 4-16 Avg. Second Order SF vs. Window size of chunk 226 .....	28
Figure 4-17 Avg. Second Order SF vs. Window size of chunk 226 .....	29
Figure 4-18 Avg. Third Order SF vs. Window size of chunk 100 .....	29

Figure 4-19 Avg. Third Order SF vs. Window size of chunk 182.....	30
Figure 4-20 Avg. Third Order SF vs. Window size of chunk 216.....	30
Figure 4-21 Avg. Third Order SF vs. Window size of chunk 228.....	31
Figure 4-22 Second order SF with Window size 6000 and lag 70 of data set 85 through 132.....	32
Figure 4-23 Second Order SF Error bar plot from data set 85 to 132 .....	32
Figure 4-24 Relative % difference of SF between successive chunks from 85 through 132 .....	33
Figure 4-26 Second Order SF Error bar plot from data set 200 to 229 .....	34
Figure 4-27 Relative % difference of SF between successive chunks from 200 through 229.....	35
Figure 4-28 Third order SF with Window size 5000 and lag 70 from data set 85 to 132	35
Figure 4-29 Error bar plot of third order SF from 200 to 229 .....	36
Figure 4-30 Third order SF with Window size 5000 and lag 70 from data set 200 to 229 .....	36
Figure 4-31 Error bar plot of third order SF from 200 to 229 .....	37



## LIST OF TABLES

Table 4-1 List of parameters required to calculate average SF .....	18
---	----

## ABBREVIATIONS

SF	Structure Function
B&W	Babcock and Wilcox
BFB	Bubbling Fluidized Bed
A/D	Analog-to-Digital
AC	Alternating Current
DC	Direct Current
PC	Personal Computer
EEPROM	Electrically Erasable Programmable Read-Only Memory
VFD	Variable Frequency Drive

# CHAPTER I

## INTRODUCTION

### 1.1 Motivation and Background

Bubbling fluidized bed are frequently used to combust biomass fuel to produce steam and electricity. The biomass fuel with its low concentration of Sulphur (S) is mixed with sand as a bed material rather than limestone. The biomass fuel contains alkali elements such as sodium and potassium in the ash. Since the alkali elements have low melting temperature compared to bed temperature this causes deposition of sodium and potassium on the surface of sand thus forming an eutectic. The softening of the surface can cause individual particle of sand to stick together to form agglomerates with a larger diameter than the individual particle of sand grains.

Fluidization quality is a function of air distribution through the bed. A well-fluidized bed provides good mass transfer of the oxygen in the air to the surface of the biomass particles to achieve good combustion. As agglomerates forms in the bed, the quality of fluidization will deteriorate and the mixing of the air and the fuel is compromised.

The quality of fluidization can be assessed by measuring the differential pressure fluctuations in the bed using a high-speed pressure transducer. A well-fluidized bed is characterized by a Gaussian distribution of the pressure fluctuations. As agglomerates form the pressure fluctuations will become more periodic which is indicative of slugging behavior. Fluidization is a highly nonlinear process with dimension around 7 [1].

Structure function (SF) has been shown to be particularly sensitive to shifts in system dynamics from chaotic to periodic.

## **1.2 Purpose**

As the agglomerates form, the fluidization quality shifts from well-mixed chaotic behavior to poorly-mixed periodic behavior. The formation of agglomerates can be managed by draining portion of the bed and controlling the accumulation of alkali below the threshold limit where the agglomerates can form. A time-averaged measure of bed pressure drop does not reveal the shift in fluidization quality. In fact, the time-averaged pressure drop across the fluidized bed could be the same whether or not agglomerates are present, or the bed is well-mixed or slugging. A method is required to detect the early onset of agglomeration so that the bed drain rate can be adjusted quickly enough to purge the accumulated alkali constituents and small agglomerates.

Previous work [2] has shown that linear and nonlinear signal analysis applied to high-speed pressure transducer measurement of bed differential pressure can be used to detect a change in fluidization quality. Linear signal analysis techniques can only provide a limited indication in bed hydrodynamics and struggle to provide an early indication of the onset of agglomeration. Nonlinear signal analysis techniques have shown greater promise, but have not been implemented commercially in a real bed-drain control scheme.

### **1.3 Goal**

The goal of this work is to show that the nonlinear structure function, when applied to a high-speed differential pressure signal, can be used to detect the early onset of agglomeration in a timely manner to be used as a control variable for the bed drain rate.

### **1.4 Objectives**

The following objectives are defined.

- Develop the necessary computer code to calculate structure function from a series of pressure measurements.
- Perform sensitivity analysis of the analysis parameters to optimize the method of bubbling bed pressure signals.
- Show the structure function can detect agglomeration in sufficient time prior to catastrophic agglomeration to allow the control system to mitigate the agglomeration and maintain well-fluidized bed.
- Show that the computation time of the calculation is fast relative to the process [3].

### **1.5 Organization**

This work is divided into 5 chapters. Chapter II provides background information on fluidized bed process, agglomeration, and details on the structure function. The third chapter describes the details of the fluidized bed set-up and data acquisition. Chapter IV details the testing performed with the proof-of-concept implementation. This thesis is concluded with the fifth chapter, which summarizes the content of this work as well as

suggestions for future research on this topic. Several appendices provide Matlab source codes used to generate the plots presented in the body of this work.

## CHAPTER II

### BACKGROUND INFORMATION

#### 2.1 Fluidized bed combustion

In the fluidized bed, fuels or biomass, especially with high sulfur, can be combusted in the air-suspended mass of particles. By controlling the temperature of the air through the bed, and also by adding reagents such as limestone, the emission of nitrogen oxide (NO<sub>x</sub>) as well as sulfur dioxide (SO<sub>2</sub>) can be controlled in an environmentally acceptable way. It is difficult to burn biomass in a traditional furnace because of its low heating value, low volatile matter, and high moisture content [4].

There are two types of fluidized beds. In the first type, the bed of particles remains in the bottom of the furnace forming well-defined region of particles and fuels such as coal wastes or biomass is fed into this bed of fluidized particles commonly known as Bubbling fluidized bed (BFB) boiler. In the other, the gas velocity through the particle is sufficiently high to lift the particles out of lower furnace and transport them to the exit of the furnace where some type of particle separator returns the particles to the bottom of the furnace. This type of fluidized bed is referred to as a circulating fluidized bed (CFB) boilers. The latter can burn a boarder range of fuels.

#### 2.2 The fluidized-bed process

When the air/gas is blown through the bed mass, it gets lifted and suspended by the air. For low air velocity, the air flowing through the inter-particle spaces is not sufficient to cause considerable motion of particles, and this state is known as fixed/static bed and is shown in figure 2-1. If the rate of gas is increased the force exerted by gas to

bed particle may counterbalance the gravitational force exerted on bed material at this state the fluidized bed just remains floating in the air. This is called fluidization condition and velocity at this state is referred to as minimum fluidization velocity. If the velocity of gas is increased further the bed particle doesn't remain uniform and the bubbles of air start to form this is called bubbling fluidized condition. A further increase in velocity of gas causes the bubbles to become large and coalesce, thus forming large voids. And at this state the mass of bed becomes interconnected to each other. This is called turbulent fluidized condition which is shown in figure 2-1. Increasing the air flow further causes bed particle to separate from container, however if the solid bed particles are separated from the container and feedback to the bed then it is known circulating fluidized bed condition.

The pressure differential between top and bottom of bed changes with respect to rate of gas/air velocity as shown in figure 2-2. For low air velocity the pressure differential slowly ramps up until the air velocity becomes equal to minimum fluidization velocity. After this point the pressure differential remains steady but at high air/gas velocity the pressure differential slowly decreases because of mass is lost from the system [5].



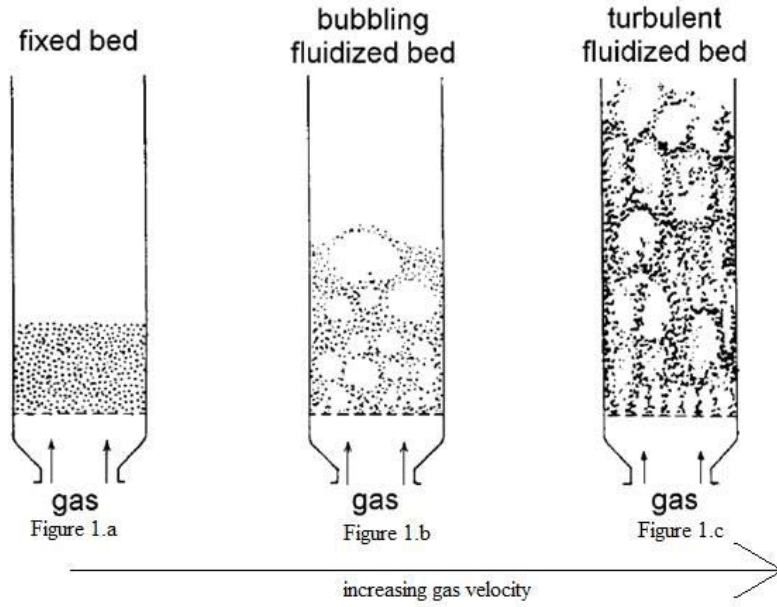


Figure 2-1 Different state of fluidized bed (adapted from [2])

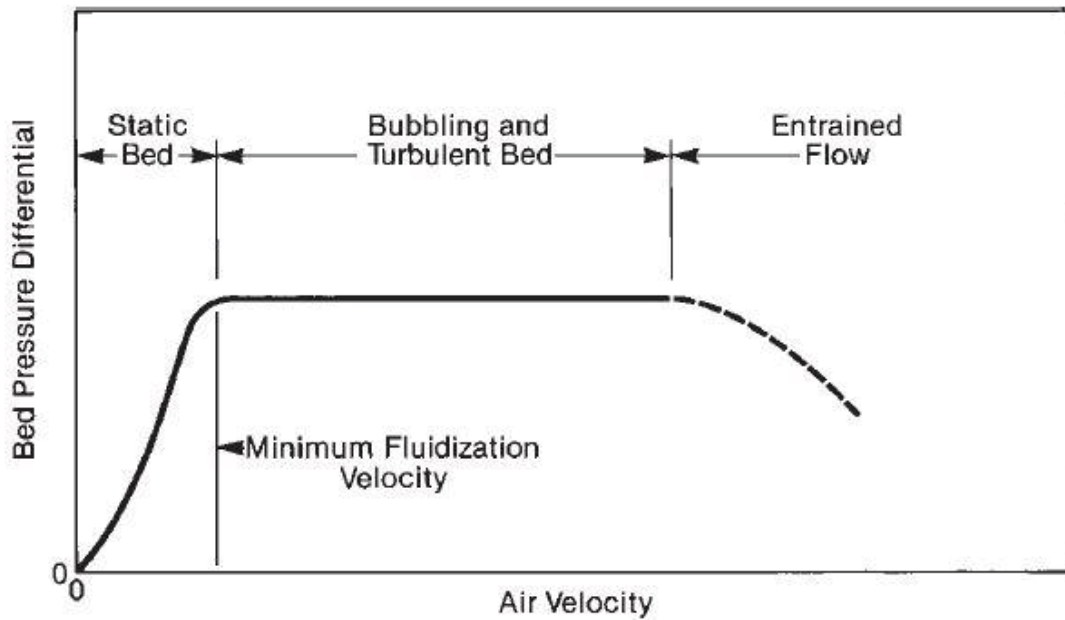


Figure 2-2 Effect of velocity on bed pressure drop (adapted from B&W, Steam)

### **2.3 Agglomeration**

During the solid fuel conversion process, alkali contained in fuel as Potassium (K) and Sodium (Na) reacts with bed material such as sand and ash, thus forming low melting alkali silicates. This causes formation of an adhesive layer around the sand particle which is sticky in nature. Due to this, the sand particles stick together forming larger agglomerates during inter-particle collision. The agglomeration is a slow process and its onset cannot be detected precisely. The formation of larger aggregates of particles lead to worse mixing, and if this process is not stopped, then eventually it results in complete defluidization of the reactor. This is one of the major operational problems because it leads to a lengthy,unscheduled, and expensive shutdown of the plant.

In industry the defluidization is controlled by observing its time scale [6]. If the time scale is long then the agglomeration can be controlled by feeding solid materials into the bed or by increasing gas velocity, which increases the overall momentum of the bed particles and thus decreasing the agglomeration tendency. The quality of the fluidization bed during normal operating conditions is characterized by a uniform temperature distribution and a stable average pressure drop. The onset of defluidization can be determined by early detection in either of these two quantities. During agglomeration, part of the bed particles will no longer be in a fluidization state. Due to this there is an average bed pressure drop.

### **2.4 Structure function and its application to non-linear time series data**

The structure function was developed to study random variables associated with random processes. The continuous random variable as a function of time  $x(t)$  is one which can take different measurement values even for the same experimental condition.

The physical process, the results of whose observations are represented by a random function, is known as a random or stochastic process. For example, when resistance of a copper wire or any element is measured, different values of resistance will be recorded which fluctuates around its mean value. Therefore, it is difficult to accurately predict the value of a random function in advance. But a range of value can always be predicted in advance.

The mathematical tools for the study stochastic functions were developed by the Soviet mathematicians A.Y. Khinchin, E.E Slutsky, and Kolmogorov. These tools are useful in the study of electric noise, velocity at a fixed point of turbulent fluid, or temperature and pressure which continuously oscillates [7].

A majority of random processes faced in real practice are best characterized as stationary process. A stationary process is one in which the value of the mean and variance remain fixed but the correlation function depends upon the difference between two times ( $t_2 - t_1$ ). A certain part of random processes for a small interval of time lag,  $\tau = t_2 - t_1$  can be considered approximately stationary but if the time under consideration is large, the mean quantities undergo significant changes and cannot be considered stationary. An important class of processes is one in which the increment  $x(t + \tau) - x(t)$  is stationary but the process  $x(t)$  is not stationary. In such a case it has finite expected value for the mean, the square, and the higher powers. The structure function (SF) becomes a useful tool in the analysis of such random processes. The structure function computes the difference between two points in a time series of values each separated by distance time lag  $\tau$ . As such it eliminates the data drift and the SF tends to converge to its ultimate shape more rapidly than the correlation function [8]. The structure function proves to be

fruitful in that case if one is uncertain that the process is stationary or not. The structure function is equivalent to the autocorrelation function. The following mathematical derivation helps to illustrate this.

The autocorrelation function is given by,

$$R(\tau) = \lim_{T \rightarrow \infty} \frac{1}{T} \int_0^T x(t)x(t + \tau)dt$$

And, the structure function is given by

$$SF(\tau) = \lim_{T \rightarrow \infty} \frac{1}{T} \int_0^T [x(t) - x(t + \tau)]^2 dt$$

In these equations  $x$  is the stationary process,  $t$  is the running time,  $\tau$  is the time lag, and  $T$  is the integration time. In experimental practice, the stationary process  $x$  is sampled at equidistant time increments and the integration is approximated by the summation given in the equation below.

$$SF(\tau) = \frac{1}{N-\tau-1} \sum_{i=1}^{N-\tau} [x(i) - x(i + \tau)]^2$$

Here,

$x(i)$  is the  $i^{\text{th}}$  sample number in the time series,  $N$  is the size of the window considered for the structure function,  $\tau$  is the difference in the number of samples for which the structure function is calculated. There exists a relationship between correlation functions and structure functions [6]. By carrying out the square under the integral, we get,

$$SF(\tau) = \lim_{T \rightarrow \infty} \frac{1}{T} \int_0^T [x(t)^2 + x(t + \tau)^2 - 2x(t)x(t + \tau)]dt$$

For a stationary processes,

The first two terms of above equation are identical at zero lag and equal to the autocorrelation function so that the equation can be written as,

$$SF(\tau) = 2R(0) - 2R(\tau)$$

From the above equation, it is clear that the zero lag terms are constants and the SF gives same information as the correlation function, the only difference being the constants, a negative sign and a factor of 2. This is only valid if the random processes under considerations are stationary and contain slow fluctuations. The detail mathematical proof of the above equations can be found in reference [7].

The correlation integral function is one of the non-linear time series tools developed by the nonlinear dynamics and chaos community. Therefore, the structure function can be used as a complement to the correlation integral method. The primary objective of time-series analysis is to obtain some quantitative information about the dynamics from a single scalar measurement. The use of single sensor data instead of multiple sensor data is one of the distinguishing features of nonlinear time-series analysis. Using surrogate data testing [9], it can be determined whether that the time-series has either chaotic dynamics or it is linear with uncorrelated noise.

After determining if the time-series has nonlinear or chaotic dynamics, the next step is to reconstruct the finite dimensional state space or phase plane of the observed system from single time series data. For this step embedding dimension and embedding time lag needs to be calculated. The embedding dimension gives the minimum number of the state space vectors that are necessary to describe the observed dynamics of the system [10]. The reconstructed attractor in phase space gives the information of stationarity and non-stationarity. From the geometrical view point, if the attractor containing the orbit does not change in the long time scale, such dynamics of the system is considered as stationary. However, if the orbit in the attractor changes, it gives important information of

system dynamics. The differential pressure data from BFB belongs to such a group. During a normal operation of the BFB, the data shows chaotic distribution, and as it approaches the onset of agglomeration the differential pressure data shows periodic distribution. That is, there is a change in data from stationary to non-stationary. The correlation integral method can be used to detect the nonlinear dynamical changes in the data. One example of the use of correlation integral method is on the compressor data to detect the onset of the stall [11].

Provenzale et al. [12] studied the applicability of distinguishing low-dimensional chaos and stochastic noise, and also described how the structure function can be used to differentiate these two cases. The structure function has been previously used by a few authors to analyze turbulence of the atmosphere.

The structure function has also been applied to the compressor data by Vhora [13] to detect the onset of stall. In his research work, he also studied the structure function in the Chua circuit, and Rossler's system, and compared the SF with bifurcation diagrams. From his analysis of structure function on those system, he showed that the structure function amplitude decreases and becomes smooth when the dynamical system is periodic but the amplitude of the structure function increases when it is chaotic.

## CHAPTER III

### B&W EXPERIMENTAL SET-UP

#### 3.1 Experimental

Bubbling fluidized bed setups have been used in this research which is a cylindrical lab-scale setup with a diameter of 2 inches. Figure 3-1 shows one example of such a lab set up. The bottom of the furnace is a BFB consisting of a semipermeable membrane of a porous sintered metal frit. This provides air distribution or fluidizing air to the bed material in the furnace. The experiment was carried out with a bed material consisting of calcined flint nominally 1100 micron topsize. The fuel consisted of a mixture of filter cake and syrup from a cellulosic ethanol production process. The fluidizing gas was a mixture of air and nitrogen resulting in a 13 % oxygen content in the bed of fluidized particles. The fluidizing gas is preheated in an annular passage along the full length of the bed to the target bed temperature with clam shell electric heaters. The bed temperature can be adjusted by adjusting the power into the clam shell electric heaters.

#### 3.2 Pressure Measurement

The bed pressure drop was measured with a differential pressure transducer (Validyne DP15-28). The pressure signal from the differential pressure sensor was then fed into a Validyne Model CD12 “High Gain Research Carrier Demodulator” which provides excitation, amplifies and demodulates the signal. The pressure fluctuations were then low pass filtered at 500 Hz and sampled at 1000 Hz to avoid aliasing effects according to the Nyquist criterion. Since the dynamics of agglomeration were all

reflected in the AC component of the signal therefore, the same signal was also high pass filtered to remove the DC offset.

The pressure data were acquired through B&W's custom data acquisition system. In this data-acquisition system, the pressure signal was sampled by using an IOtech A/D converter and then subsequently filtered by a filter card with a 500 Hz low pass and 1 Hz high pass digital filter. The sampling frequency was kept constant during the entire experiment. Time series of bed pressure drop and local pressure fluctuations were stored on a Laptop PC with custom software for data storage.





Figure 3-1 Fluidized-bed experimental set-up

### 3.3 Data Collection

The data were collected for about 8 hours and 25 minutes, the data were sampled for 120 seconds followed by approximately 12 seconds of analysis, and the collection of the next block of data was carried out. For each sampled data of 120 seconds (chunk), a separate folder was created where all the 120 seconds samples of data were stored in .wav format. Altogether there were 231 data sets collected.

During the experiment, the bed alkali concentration was estimated to be 1.5 % based on total fuel fired. The BFB's reactor was heated initially to 700°C in N<sub>2</sub> (reducing atmosphere) at 07:55 AM. The fluidized bed was heated at the rate of 1°C/min in N<sub>2</sub>. The bed was first agglomerated when the temperature was 815°C at time 12:48 PM which is also the collection of data set number 132. Also, the agglomeration was noted at several other points during the experiment. A metal rod was used to manually mix up bed material to get it suspended after agglomeration event, and the experiment was continued.

## CHAPTER IV

### RESULTS AND DISCUSSIONS

#### 4.1 Application of Structure Function to BFB Differential Pressure Time Series

The structure function is calculated for both raw and filtered data. The time series data is divided into windows consisting of  $N$  sample points. In each window, a structure function value is calculated for a fixed time lag. The structure function can be calculated for overlapping or non-overlapping windows. Unlike power spectral analysis, the structure function does not have the problem of windowing or aliasing [14]. Before calculating the structure function, the time-series data are filtered with a sampling frequency of 120 Hz and normalized along its average value per data set or chunk. The Matlab code to filter and normalize data is given in Program 2 and Program 3 respectively in the Appendix. The plot of raw data as well as filtered and normalized data are shown in Figure 4-1 and Figure 4-2, respectively. The Matlab code to plot the general structure function is given in the Program 1 of the Appendix section. Figure 4-3 shows one example plot of the structure function obtained from the BFB's time-series. For this plot an arbitrary window size of 4000 samples and a time-lag of 70 samples was chosen.

The structure function plot can be represented by using its average value and standard deviation as shown in Figure 4-4. The table 4-1 gives a glimpse of how the average value of structure functions are obtained. After total no. of structure function is obtained for a particular chunk for fixed time lag and fixed window, the average and standard deviation is taken for total no. of structure function value per chunk. And, just a

single value of average structure function gives the information of how the structure function value fluctuates in that particular chunk.

Table 4-1 List of parameters required to calculate average SF

Number of samples in each dataset	120,000 samples = 1 chunk = 2 minutes
Sampling frequency	1000 Hz
Window size	4000 samples = 4 seconds
Time-lag	70 samples
No. of structure function obtained	$120,000/4000 = 30$ number of windows

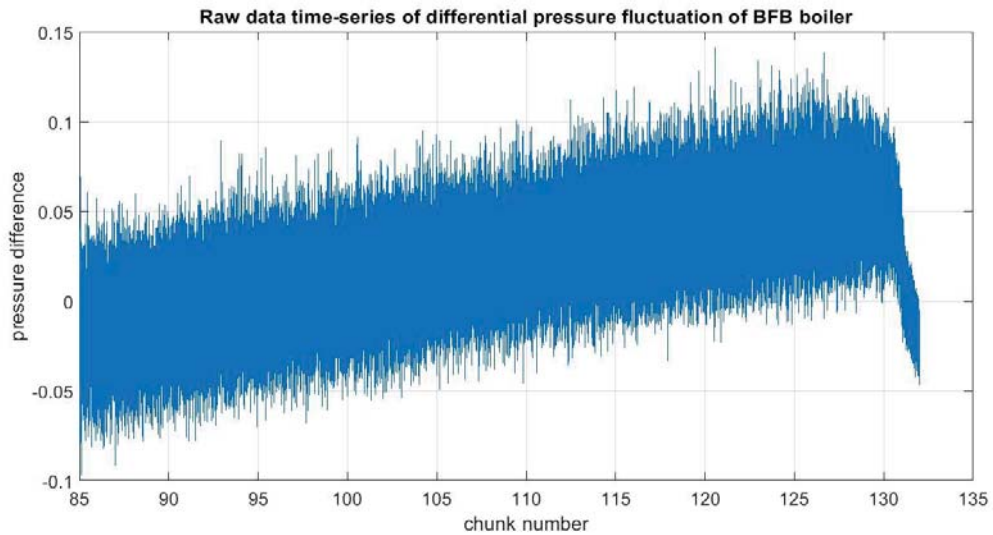


Figure 4-1 time-series plot of differential pressure fluctuations

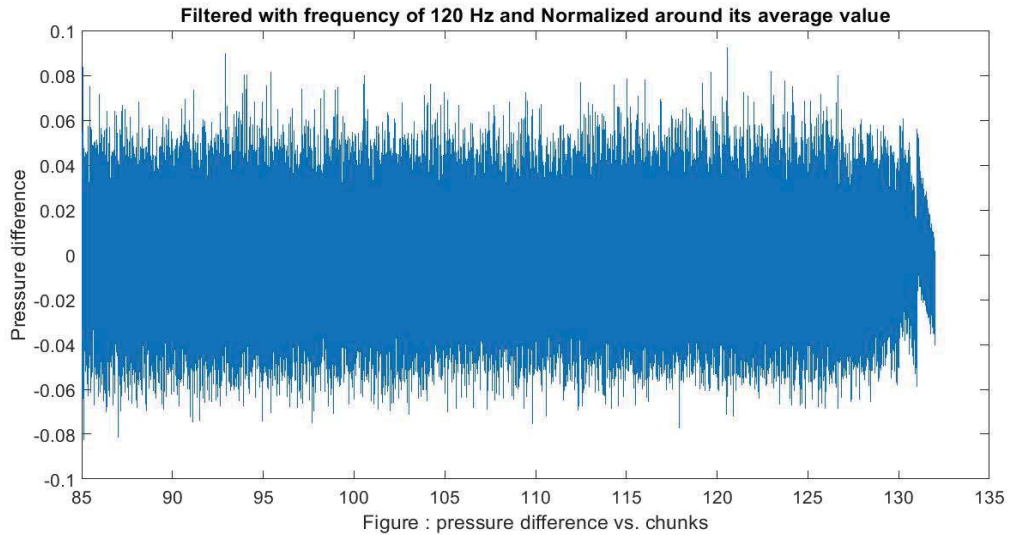


Figure 4-2 Filtered with butterworth filter and normalized around central mean

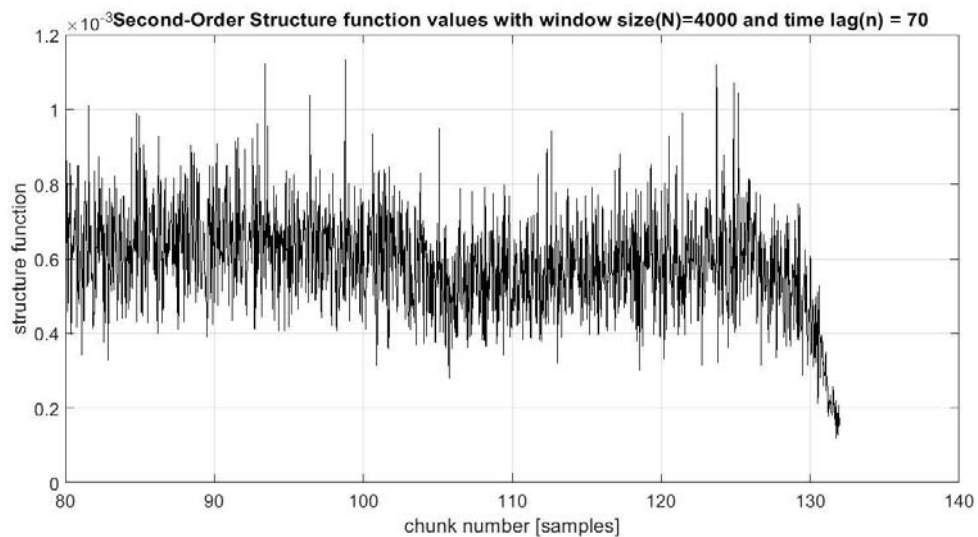


Figure 4-3 Second order SF with window size of 4000 and lag 70

Since it is difficult to interpret the graph obtained as shown in Figure 4-3. The structure function plot can be represented by using its average value and standard deviation as shown in Figure 4-4. Therefore, the average value of structure function is calculated for 30 number of structure function. In addition to this, the standard deviation for 30 number of structure function is also calculated. So just one value of average

structure function and its standard deviation gives all the information of structure function in that particular set of data.

The number of structure function obtained from a single dataset may vary depending upon the size of window selected. Since the value of structure function depends upon time-lag and window size, it is always desired to do sensitivity analysis with respect to both of these two values.

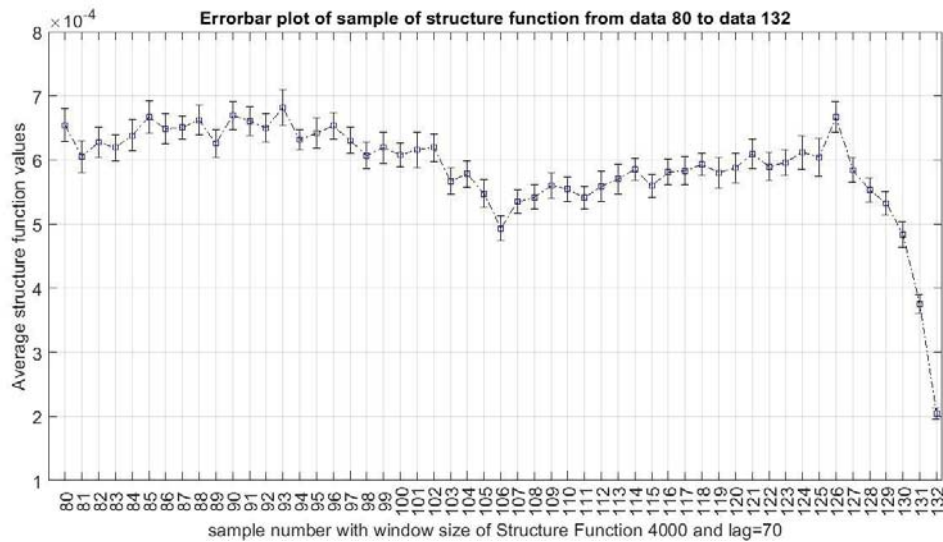


Figure 4-4 Error bar plot of Second order SF with window size 4000 and lag 70

#### 4.2 Sensitivity Analysis of Structure Function with respect to Time-lag

The average structure function is calculated for different values of time-lag in each window. For this analysis, an arbitrary value of Window size 4000 is chosen. A typical Matlab code to generate average SF versus timelag is given in Program 1 in the Appendix. Figure 4-5 shows the plot of average SF vs time-lag. From the plot it is clear that the peak value lies in the range of 70 to 130. The peak time lag is chosen as the optimum time lag since the peak time lag gives maximum information about the signal

[13]. As seen from the plot in Figures 4-5,4-6, 4-7, 4-8 and 4-9, for low values of time lag it gives information about the noise in the signal. The analysis is done with the second-order and third-order structure function.

Figure 4-10, 4-11, 4-12, and 4-13 shows time lag versus average third-order structure function. The peak value of the average structure function is in the range between 70 to 130.

Therefore, we choose time lag of 70 for both second order and third order structure function because near agglomeration the structure function peak occurs at lower values of  $\tau$  ( $\tau \approx 70$ ). For example, in Figure 4-8, note that the peak occurs at  $\tau \approx 70$  for chunk no. 133.

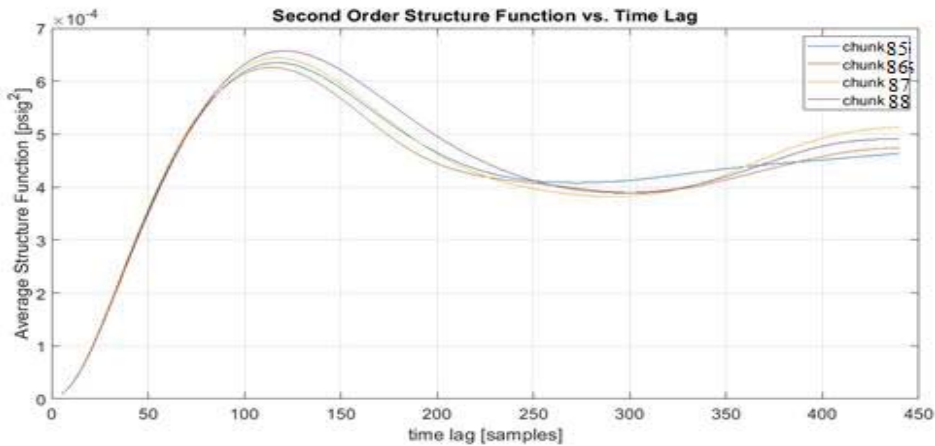


Figure 4-5 Average 2<sup>nd</sup> order SF vs. time lag for Chunk 85, 86, 87, 88

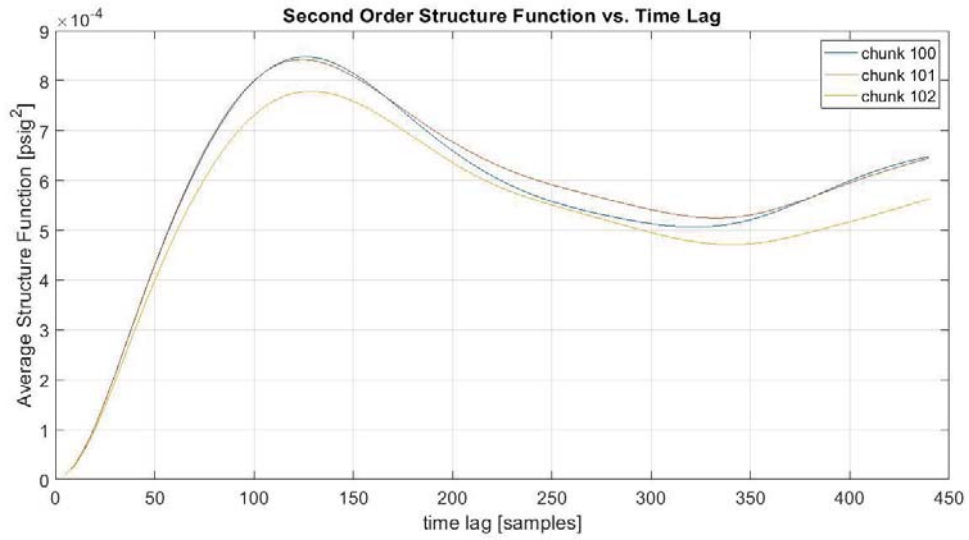


Figure 4-6 Average 2<sup>nd</sup> order Sf Vs. time lag for chunk 100, 101, 102, 103

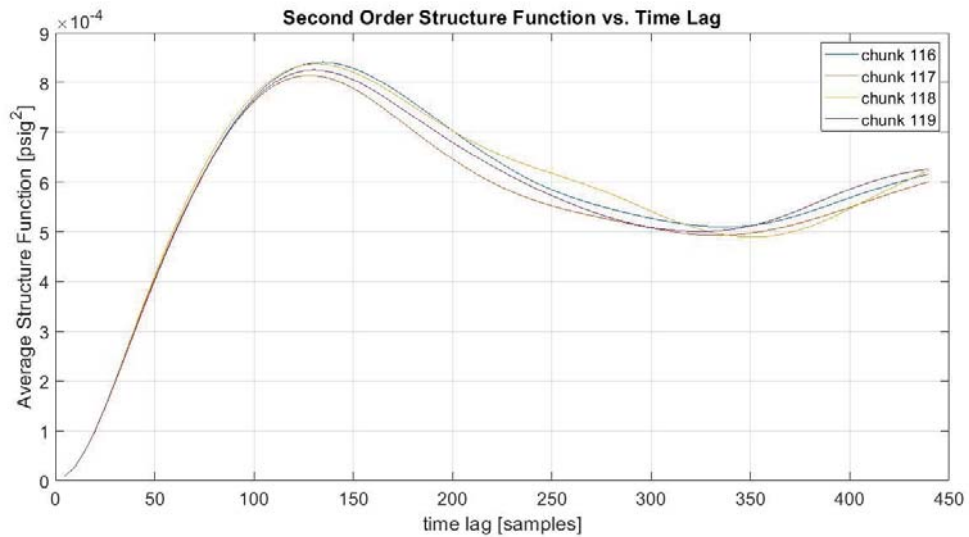


Figure 4-7 Average 2<sup>nd</sup> order SF vs. time lag of chunk 116, 117, 118, 119

Also, it can be seen from the Figure 4-8, 4-9, 4-11, and 4-13 that as the time-series data approaches agglomeration, the peak is obtained for lower values of time-lag,



and also the average value of structure function is decreased. This gives information about change in time series from a chaotic distribution to a periodic distribution.

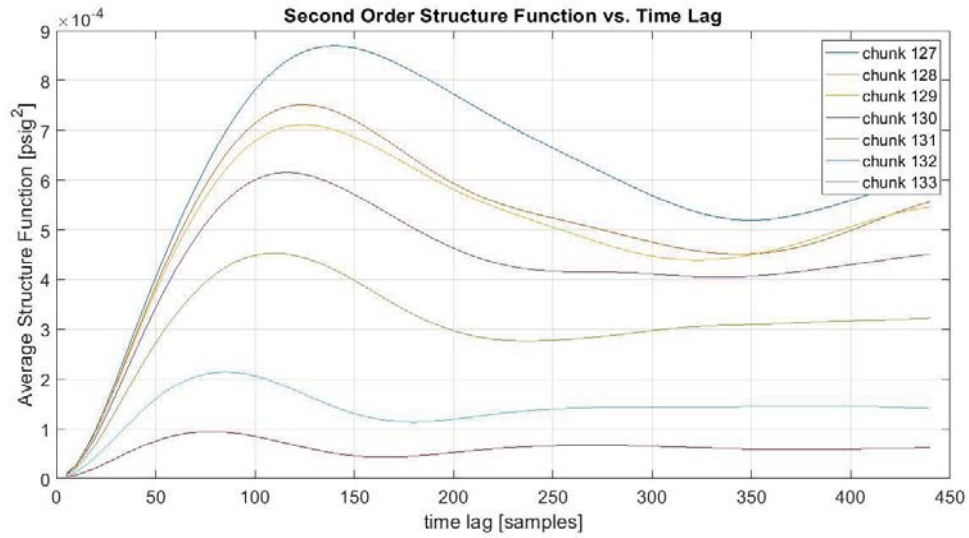


Figure 4-8 Average 2<sup>nd</sup> order SF vs. time lag of chunk 127 to chunk 133

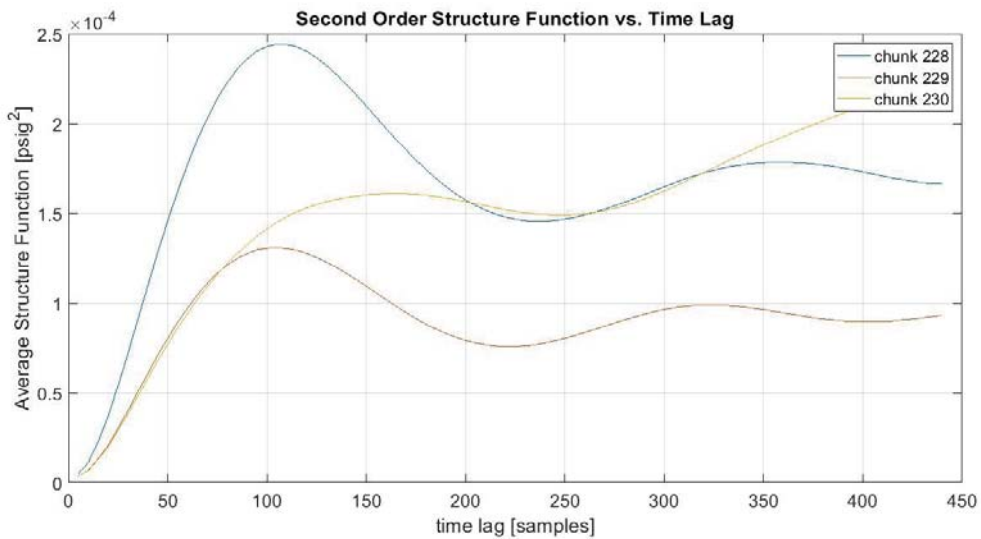


Figure 4-9 Average 2<sup>nd</sup> order SF vs. time lag of chunk 228, 229, 230

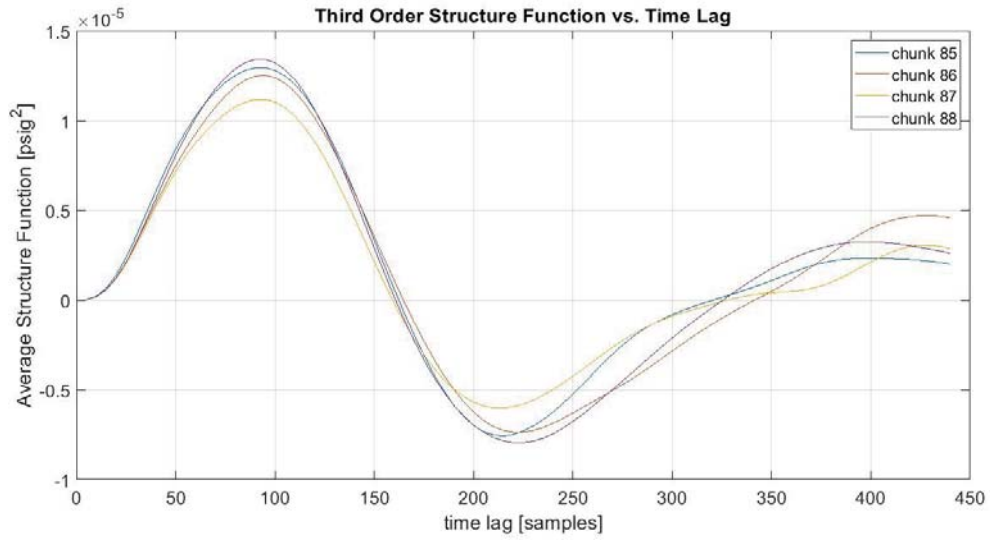


Figure 4-10 Average 3<sup>rd</sup> Order SF vs. time lag of chunk 85, 86, 87, 88

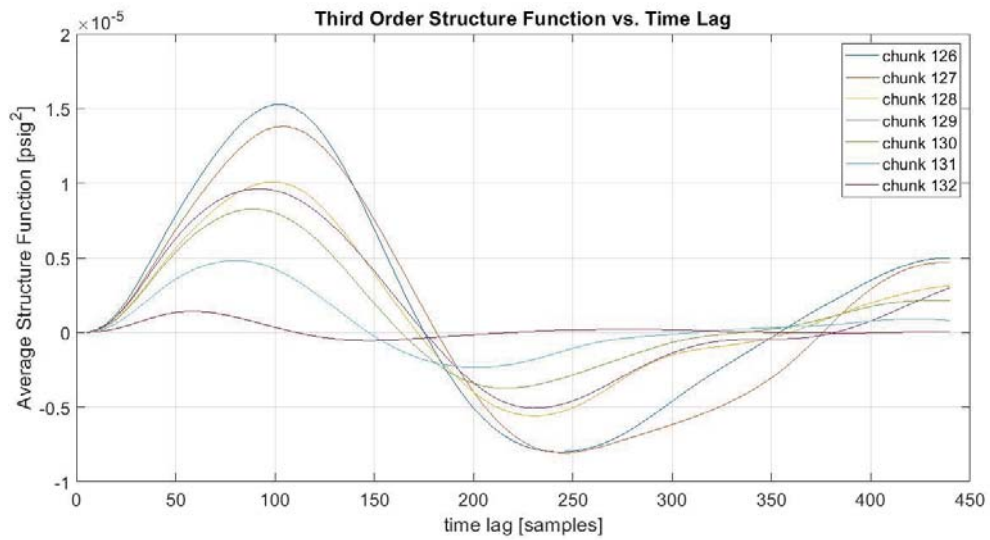


Figure 4-11 Average 3<sup>rd</sup> order SF vs. time lag of chunk 126 through 132

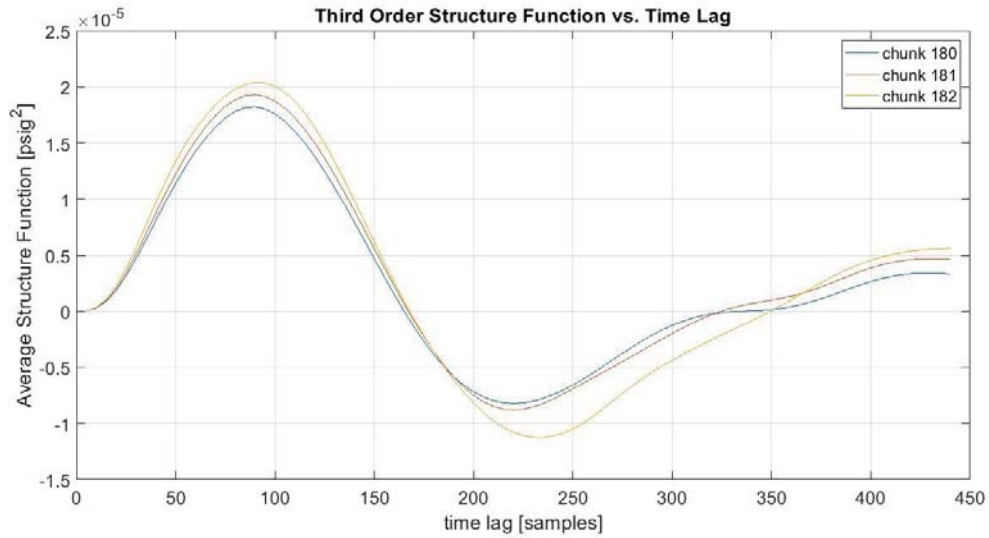


Figure 4-12 Average 3<sup>rd</sup> order SF vs. time lag of chunk 180, 181, and 182

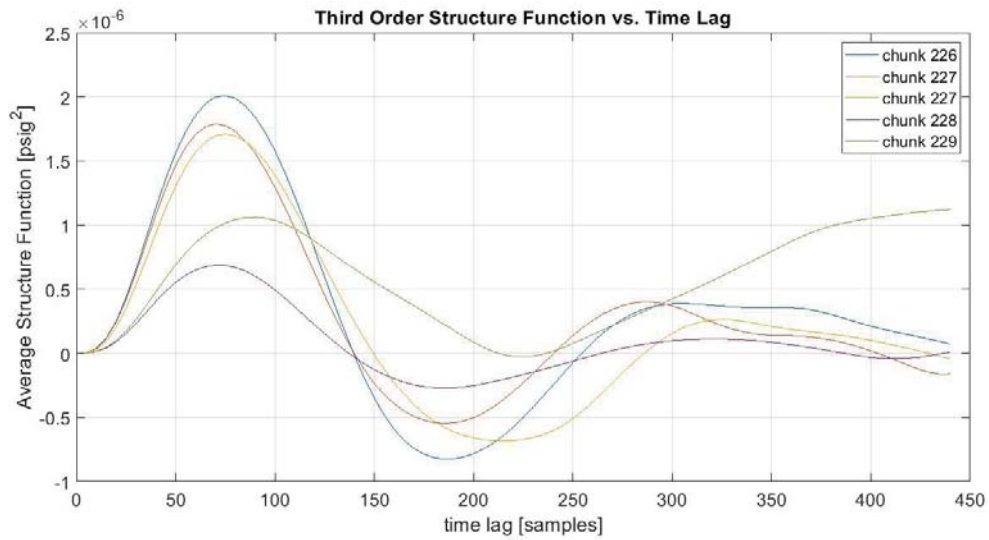


Figure 4-13 Average 3<sup>rd</sup> order SF vs. time lag of chunk 226 through 230

### 4.3 Sensitivity Analysis of Structure function with respect to window size

The average value of the structure function is plotted with respect to the window size. A typical Matlab code to plot the SF vs. window size is given in program 6 of the Appendix. The Figure 4-14 shows one example of such a plot.

From the Figure 4-15, 4-16, 4-17, and 4-18, it seems that for window sizes less than 5000 the curve is reminiscent of a transient. However, for larger windows, the value of the average structure function becomes nearly constant. The analysis is done with a second order structure function for dataset numbers 85 and 86 respectively.

We have also done the analysis using a third order SF. As shown in Figure 4-20, 4-21, 4-22, and 4-23 shows the plot of window size vs. third order SF with the different data sets. It seems that the structure function is independent of window size beyond 6000 (2<sup>nd</sup> order) – 5000 (3<sup>rd</sup> order) window size, and such window sizes selected do a better job of capturing the fluidized bed dynamics.

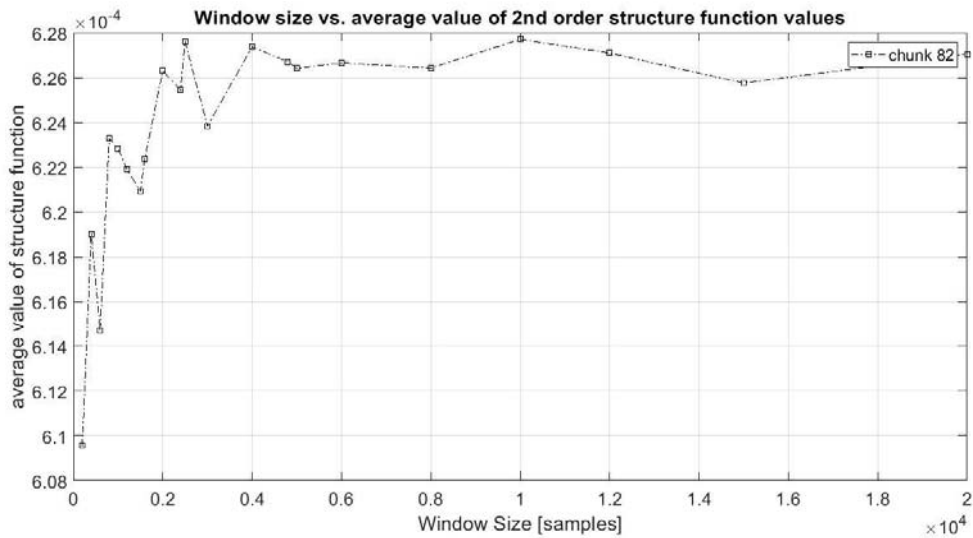


Figure 4-14 Avg. Second Order SF vs Window size of chunk 82

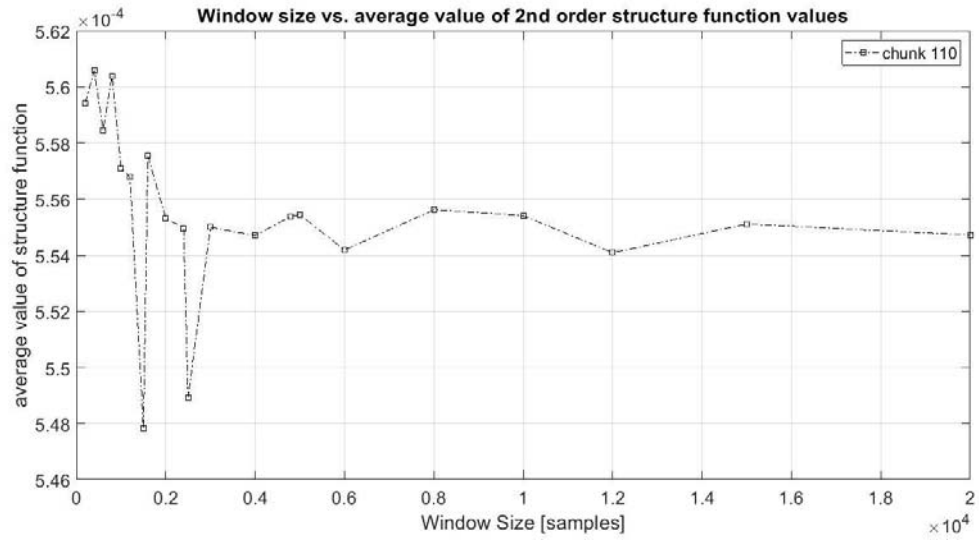


Figure 4-15 Avg. Second Order SF vs Window size of chunk 110

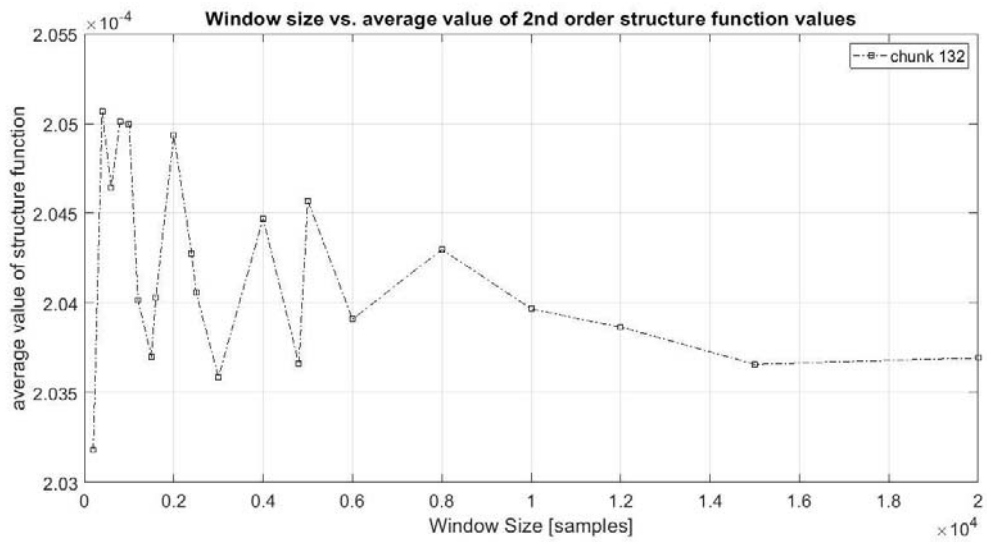


Figure 4-16 Avg. Second Order SF vs Window size of chunk 132

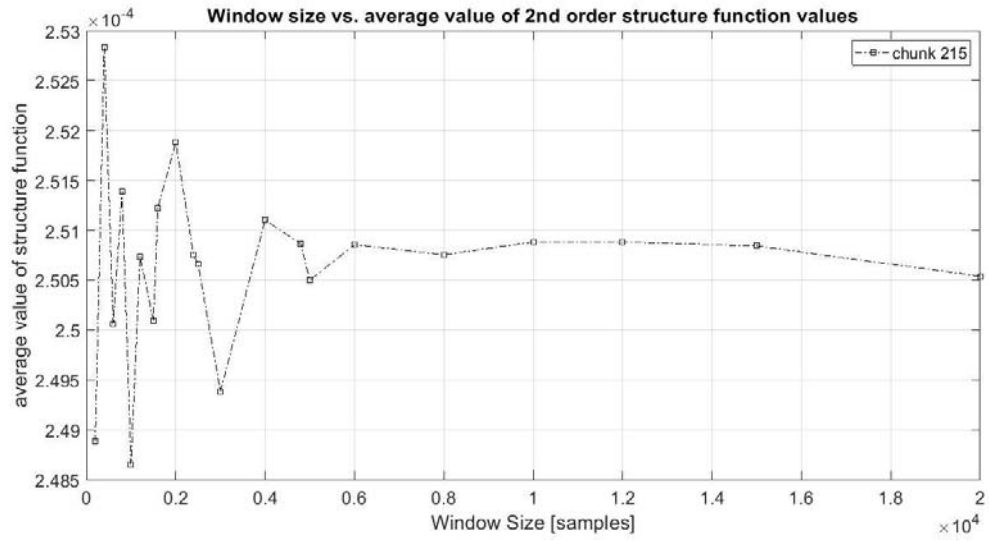


Figure 4-17 Avg. Second Order SF vs. Window size of chunk 215

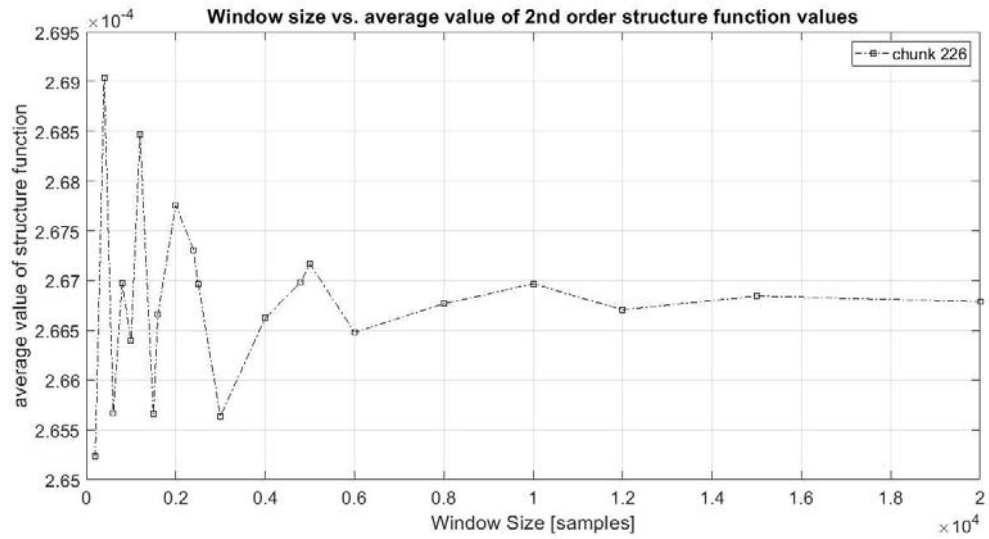


Figure 4-18 Avg. Second Order SF vs. Window size of chunk 226

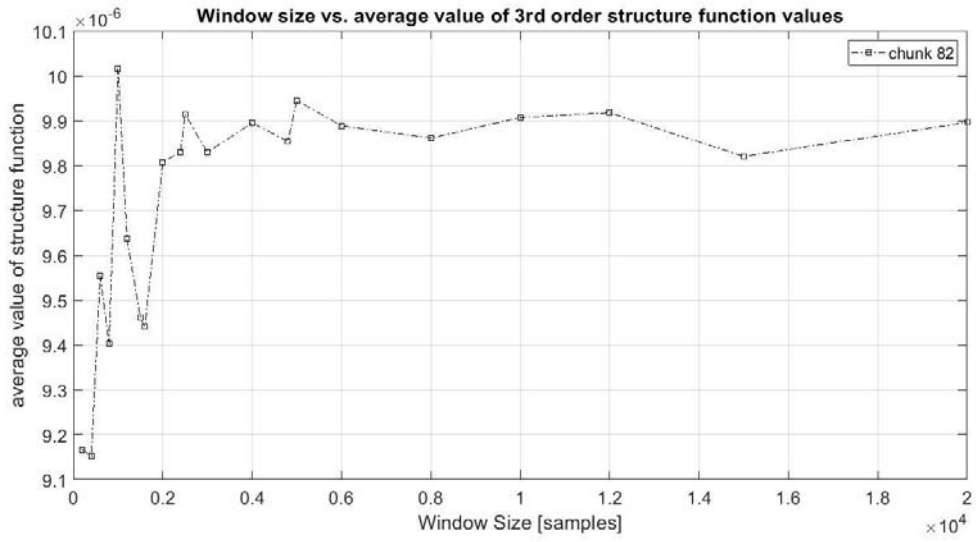


Figure 4-19 Avg. Second Order SF vs. Window size of chunk 226

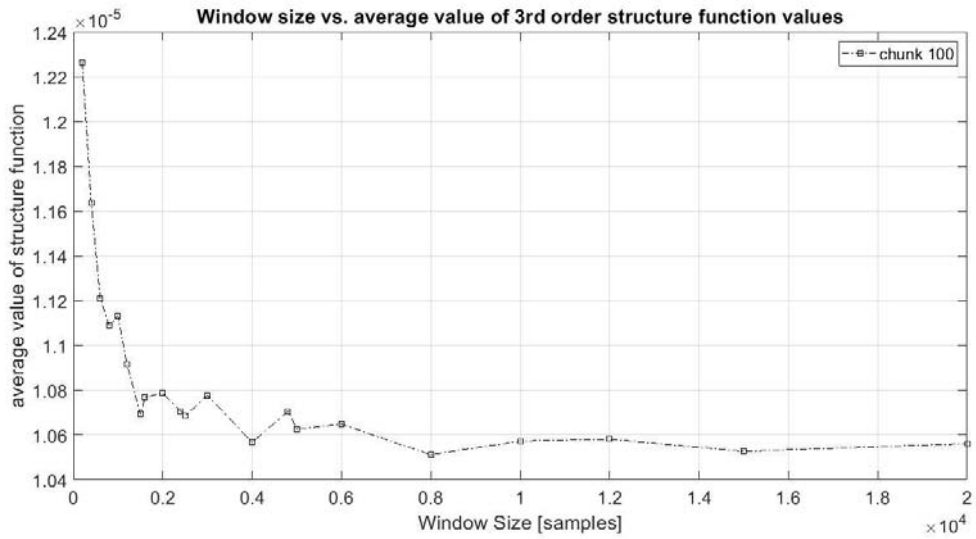


Figure 4-20 Avg. Third Order SF vs. Window size of chunk 100

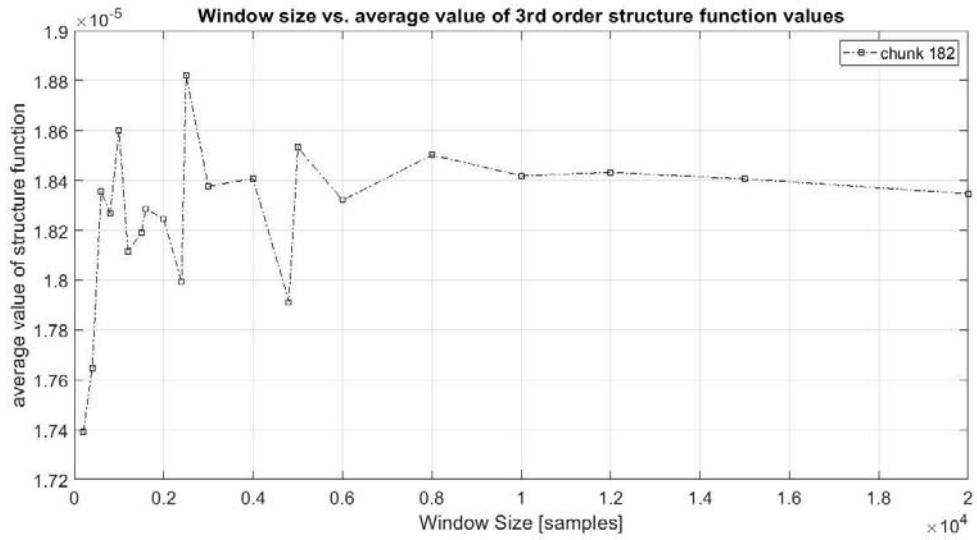


Figure 4-21 Avg. Third Order SF vs. Window size of chunk 182

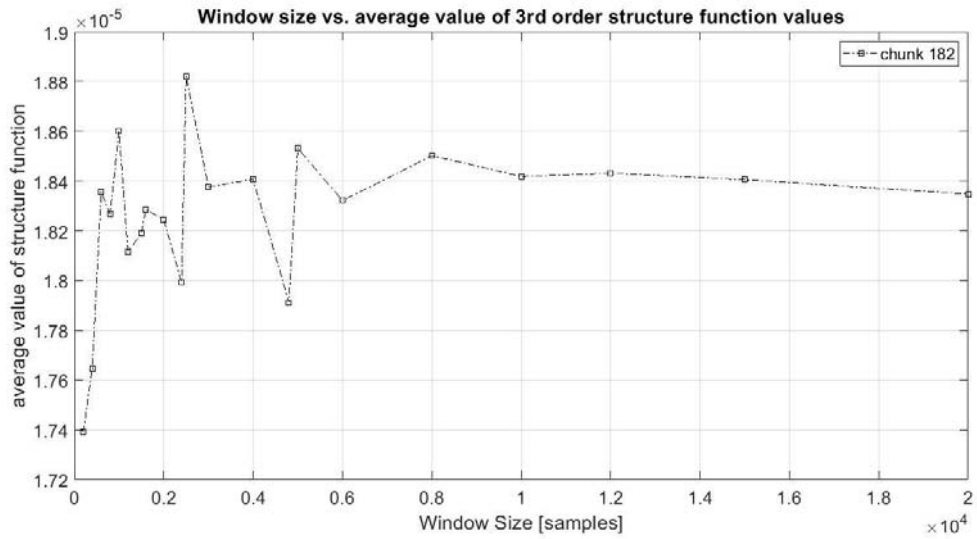


Figure 4-22 Avg. Third Order SF vs. Window size of chunk 216



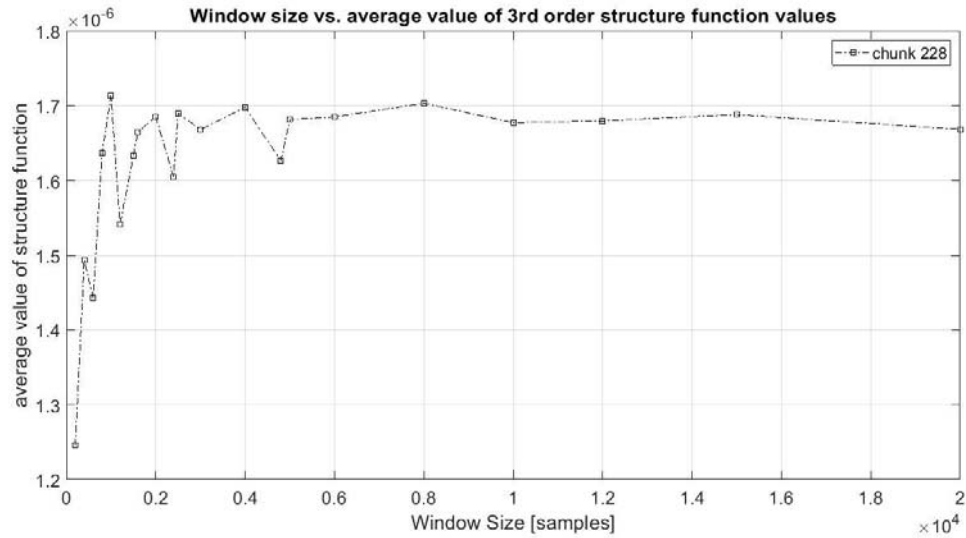


Figure 4-23 Avg. Third Order SF vs. Window size of chunk 228

#### 4.4 Structure function applied to BFB data

The second order structure function is applied to the filtered and normalized datasets from 85 to 132. These datasets consist of time-series of chaotic and periodic distributions of data. As seen in the figure 4-24, as the sample approaches dataset 132 the differential pressure fluctuation gets ramps down. At this state, the fluid bed dynamics shows periodic distribution of bed differential pressure measurements. The objective is to use the structure function and see if it detects agglomeration or defluidization before the average pressure drop analysis.

We choose a second order structure function with Window size of 6000 and time-lag of 70 samples for the analysis. The figure 4-25 is an example of such a plot. From the figure it is obvious that after chunk number 126, the trend of the average of the structure function ramps down. This gives good information about what is happening in the fluidized bed dynamics that is, there is a change in bed pressure dynamics from a chaotic distribution to a periodic distribution. As the data becomes a periodic distribution the

structure function becomes smooth, and its amplitude decreases. The Matlab code to generate the Average structure function with standard deviation as errorbar is given in Program 8 of the Appendix.

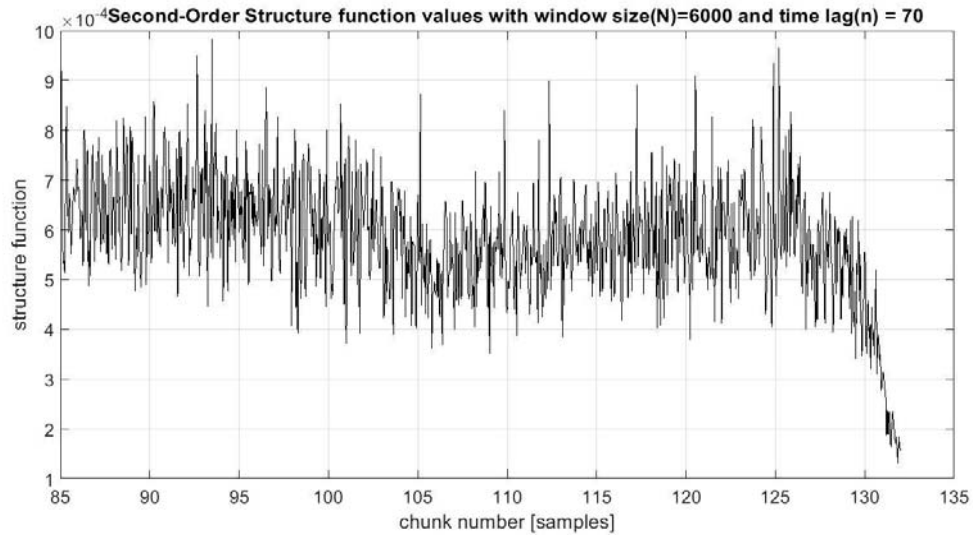


Figure 4-24 Second order SF with Window size 6000 and lag 70 of data set 85 through 132

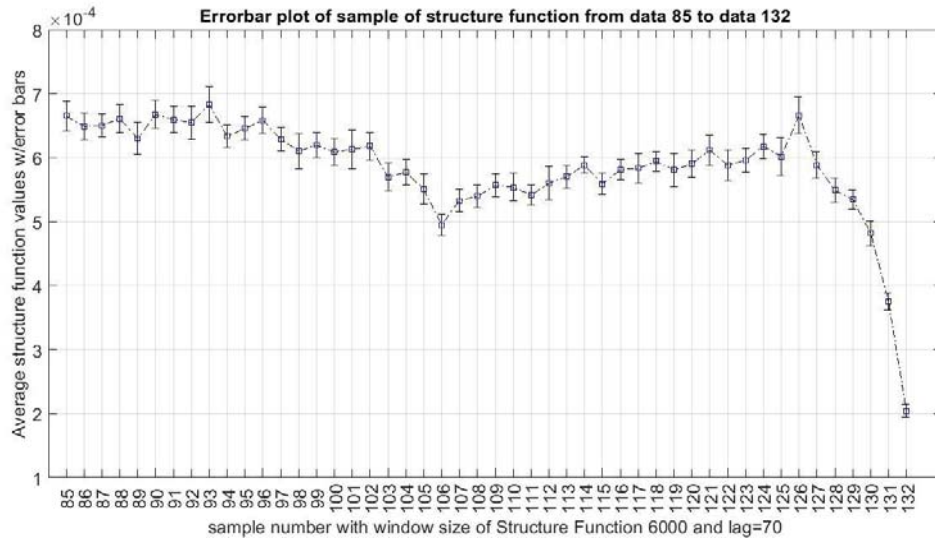


Figure 4-25 Second Order SF Error bar plot from data set 85 to 132

**Relative % difference of 2nd Order SF consecutive chunks**

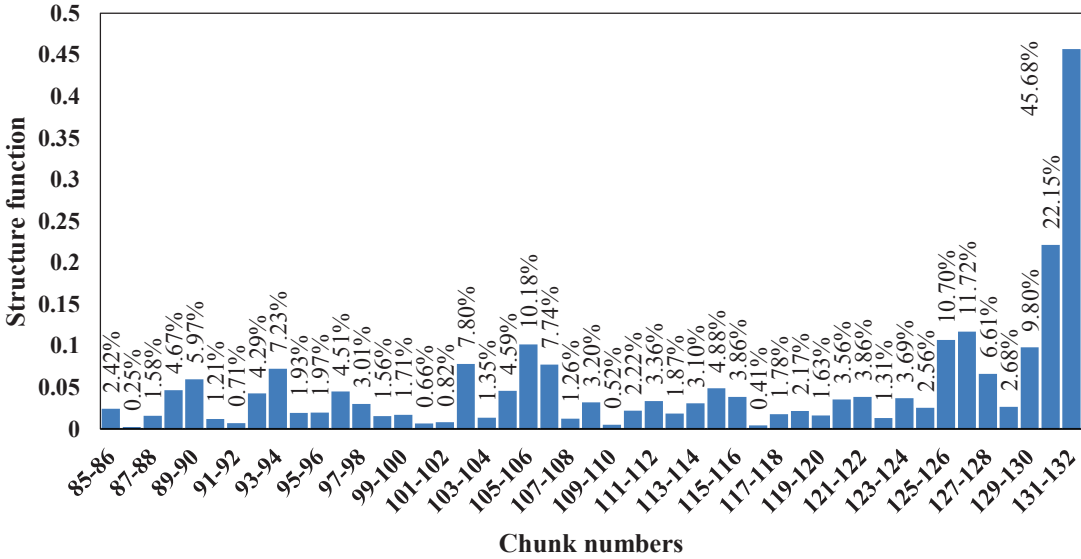


Figure 4-26 Relative % difference of SF between successive chunks from 85 through 132

Another set of data from 200 to 229 is tested again using the second order structure function. Figure 4-25 and 4-26 shows the plot of 2<sup>nd</sup> order SF with window size of 6000 and lag 70.

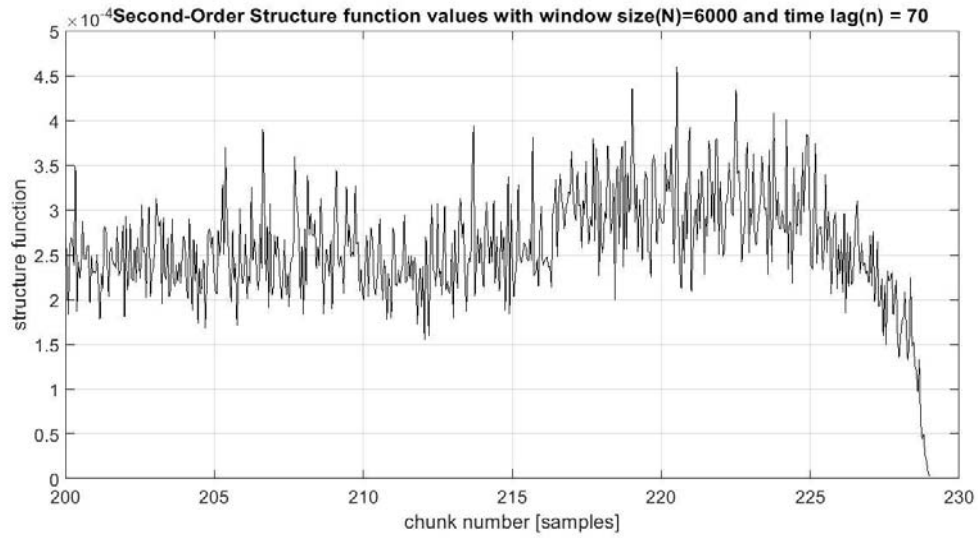


Figure 4-27 Second order SF with Window size 6000 and lag 70 of data set 200 to 229

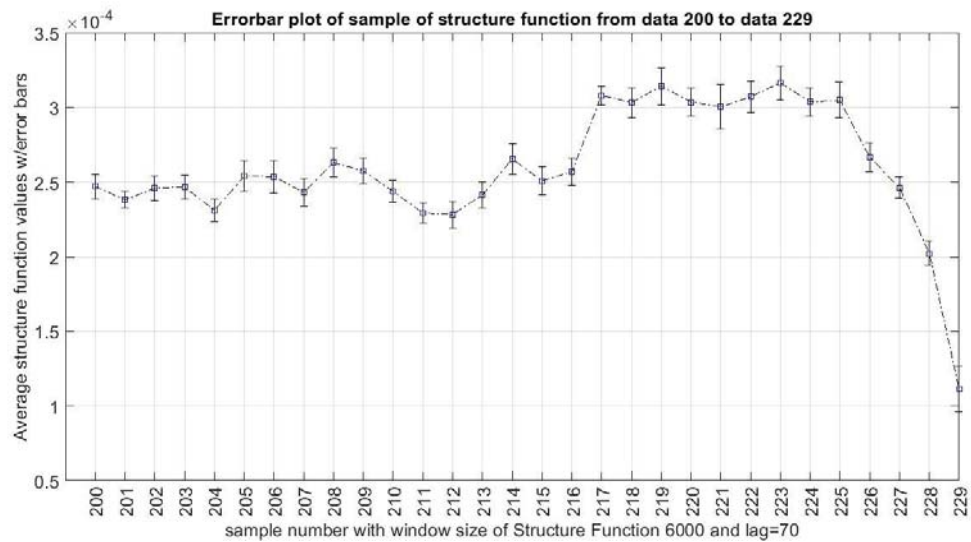


Figure 4-28 Second Order SF Error bar plot from data set 200 to 229

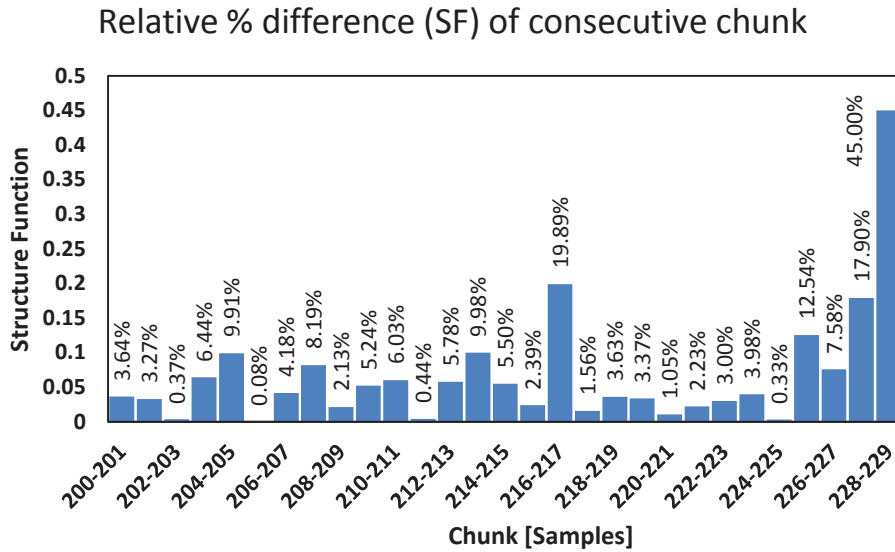


Figure 4-29 Relative % difference of SF between successive chunks from 200 through 229

Again, a third order structure function is used to do the analysis of data from 85 to 132 and data set from 200 to 229. The sequential window size of 5000 samples and time-lag of 70 samples is chosen. Figure 4-28, 4-29, 4-30, 4-31 shows plot of such a SF.

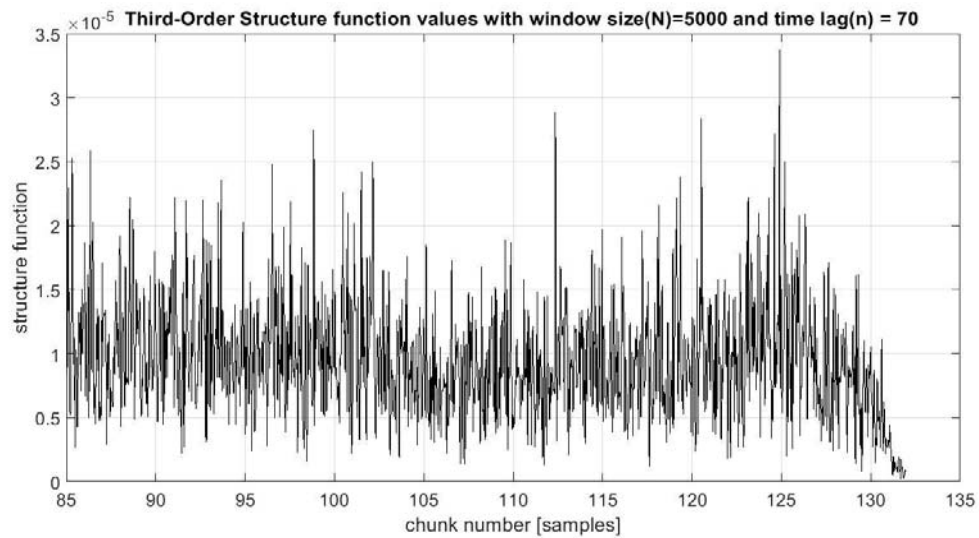


Figure 4-30 Third order SF with Window size 5000 and lag 70 from data set 85 to 132

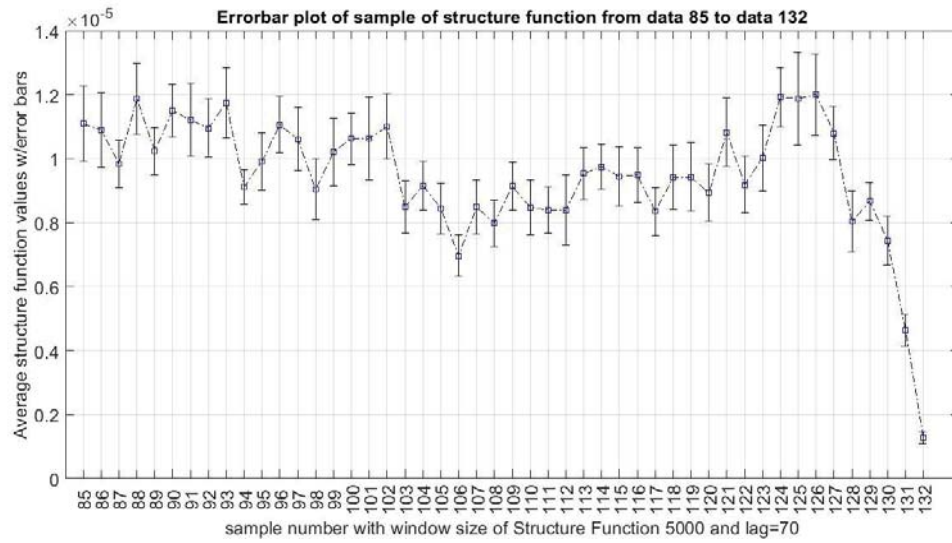


Figure 4-31 Error bar plot of third order SF from 200 to 229

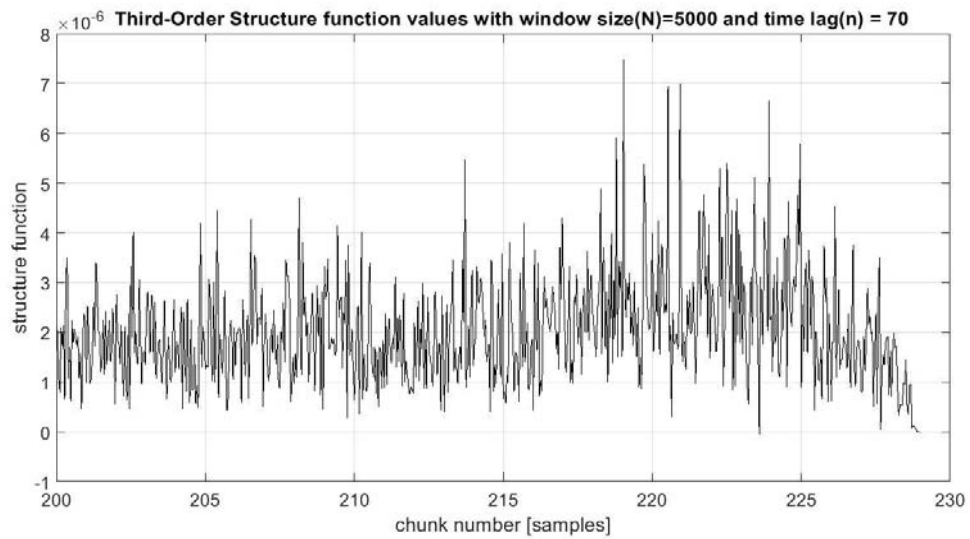


Figure 4-32 Third order SF with Window size 5000 and lag 70 from data set 200 to 229

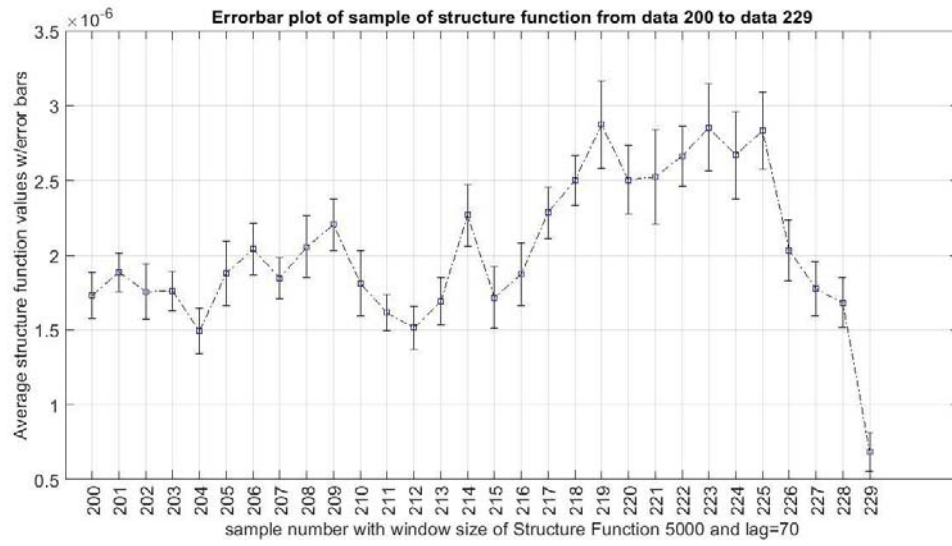


Figure 4-33 Error bar plot of third order SF from 200 to 229

## **CHAPTER V**

### **CONCLUSION**

The structure function shows that as the bed material begins to agglomerate, the structure function value drops. This is indicative of the system shifting from random or stochastic to periodic processes. This is consistent with the expectation that as the bed material agglomerates the pressure fluctuations shift from a Gaussian distribution to a periodic distribution, i.e., a shift in the nature of the hydrodynamics or a drift in stationarity.

The bed drain system of a fluidized bed has been designed to remove 10% of the bed inventory in one hour. The alkali content of the bed must be kept below 5% by weight according to B&W's general rule of thumb. If the percentage weight of alkali were to increase to 6% and incipient agglomeration occurs, then the analysis needs to detect the onset of agglomeration approximately no faster than 6 minutes ahead of the need for action according to the B&W research group. This assumes the drain rate was fast compared with the accumulation rate of alkali. In 6 minutes the concentration of alkali can be restored to a safe level. From the data analysis, as shown in the figure 4-26 and 4-29 which shows the percentage difference between consecutive chunks, so far only a 10% to 15% shift in structure function value indicates a shift in system dynamics, and this provides adequate sensitivity to detect the onset of agglomeration in a timely manner. The structure function is robust in detecting the onset of agglomeration. Even though the



structure function has been extensively used by the turbulence community, this is the first application of it on the detection of onset of agglomeration.

Since the analysis parameters can be significantly reduced to reduce the computation time and computing capacity, the technique lends itself to programming on an EPROM chip associated with VFD of bed drain screw or into the FocalPoint Optimizer.

The structure function algorithm seems to be an accurate agglomeration warning algorithm that has been tested, in an off-line manner in this research work. The structure function investigation applied to the BFB time-series data has given promising results. However studies using overlapping window, and structure function analysis in frequency domain may give more insights of a BFB dynamics which is left as a future work.

## REFERENCES

- [1] A. M. Fraser and H. L. Swinney, “Independent coordinates for strange attractors from mutual information,” *Phys. Rev. A*, vol. 33, no. 2, p. 1134, 1986.
- [2] M. Öhman, A. Nordin, B.-J. Skrifvars, R. Backman, and M. Hupa, “Bed Agglomeration Characteristics during Fluidized Bed Combustion of Biomass Fuels,” *Energy Fuels*, vol. 14, no. 1, pp. 169–178, Jan. 2000.
- [3] “Private Correspondence with Thomas J. Flynn at The Babcock & Wilcox Company,” 25-Jun-2018.
- [4] *Steam, Its Generation and Use*. Babcock & Wilcox., 1913.
- [5] M. Bartels, “Agglomeration in fluidized beds: Detection and counteraction,” 2008.
- [6] “Agglomeration in fluidized beds at high temperatures: Mechanisms, detection and prevention,” *Prog. Energy Combust. Sci.*, vol. 34, no. 5, pp. 633–666, Oct. 2008.
- [7] S. Panchev, *Random Functions and Turbulence: International Series of Monographs in Natural Philosophy*. Elsevier, 2016.
- [8] E. O. Schulz-DuBois and I. Rehberg, “Structure function in lieu of correlation function,” *Appl. Phys.*, vol. 24, no. 4, pp. 323–329, Apr. 1981.
- [9] J. Theiler, S. Eubank, A. Longtin, B. Galdrikian, and J. Dooyne Farmer, “Testing for nonlinearity in time series: the method of surrogate data,” *Phys. Nonlinear Phenom.*, vol. 58, no. 1, pp. 77–94, Sep. 1992.
- [10] M. B. Kennel, R. Brown, and H. D. I. Abarbanel, “Determining embedding dimension for phase-space reconstruction using a geometrical construction,” *Phys. Rev. A*, vol. 45, no. 6, pp. 3403–3411, Mar. 1992.

- [11] M. M. Bright, H. K. Qammar, and L. Wang, “Investigation of Pre-stall Mode and Pip Inception in High-Speed Compressors Through the Use of Correlation Integral,” *J. Turbomach.*, vol. 121, no. 4, pp. 743–750, Oct. 1999.
- [12] A. Provenzale, L. A. Smith, R. Vio, and G. Murante, “Distinguishing between low-dimensional dynamics and randomness in measured time series,” *Phys. Nonlinear Phenom.*, vol. 58, no. 1, pp. 31–49, Sep. 1992.
- [13] Vhora, Mohamad Hanif, *Detection of Stall Precursors in High Speed Axial Flow Compressors Using Structure Function Analysis Technique*. 1998.
- [14] M. Lainela and E. Valtaoja, “Structure Function Analysis of High Radio Frequency Variability in the Metsaehovi Monitoring Sample of Active Galactic Nuclei,” *Astrophys. J.*, vol. 416, p. 485, Oct. 1993.

## **APPENDICES**

## Appendix 1

### 1. PROGRAM 1 GENERAL SECOND ORDER STRUCTURE FUNCTION

```
function [jk,yy,sf_out] =st_structure_fcn(x, N, n)
% Matlab function to calculate Structure Function, Usage:
%
%       [sf_out] = st_structure_fcn(x, N, n)
% where
% x = Data column vector for which structure function is calculated
% N = windows length for which SF is calculateds
% n = delay within window N for SF Calculations (n < N)
% SF= the structure function output;
% Note that this version pretain to non-overlapping windows
% F.M.

%*****
%*****

k=1;
Nx=length(x);
ii=fix(Nx/N);      % number of windows of length N in x
sf_out=zeros(ii,1); % which is also the number of SF caculated
for i=0:ii-1
    temp1=x(i*N+n+1:i*N+N,:)-x(i*N+1:i*N+N-n,:);

    yy(:,k) = mean(temp1.^2);
    sf_out(i+1)=mean(temp1.^2);
    k=k+1;
end
i=0:ii-1;
jk = linspace(85,132,length(i));

%*****
%*****

figure(1)
plot(jk,sf_out,'k')

title(sprintf('Structure function with window size(N)=%d and time lag(n) =
%d',N,n),'fontsize',16);
xlabel('chunk number [samples]','fontsize',16);
ylabel('structure function (psig^{2})','Interpreter','tex','fontsize',16);
grid on;
```

## Appendix 2

### 2. PROGRAM 2 FILTERING OF RAW DATA

```
%filtering of raw data with sampling frequency of 120 Hz
%Using 16 order butterworth filter
clear y1
clear xData1
clear xN
N1=85; % dataset number 85 corresponds to chaotic distribution
N2=132; %dataset 132 corresponds to periodic distribution
sampling_freq = 1000;
nyq_freq = sampling_freq/2; % nyquist sampling frequency

fc = 120; %cut-off frequency

wn = fc/nyq_freq;
[b,a] = butter(16,wn,'low');
%
k1=1;
for i=N1:N2
y1(:,k1) = filtfilt(b,a,data{i}{1});
k1=k1+1;
end
%end of the program
```

## Appendix 3

### 3. PROGRAM 3 NORMALIZATION OF FILTERED DATA

```
%%  
%Normalization of data  
k=1;  
xDat = y1; %y1 is filtered data  
nl = size(y1);  
nl =nl(:,2); % length of time series  
for j=1:nl  
    xDat_mean = mean(xDat(:,j)); % calculates mean  
    xDat_var = var(xDat(:,j)); %calculates variance  
    xDat_std = std(xDat(:,j)); %calculates standard deviation  
    xNorm(:,j)= (xDat(:,j)-xDat_mean); %normalized around central mean per chunk  
    Xscale(:,j) =(xDat(:,j)-xDat_mean);  
  
end  
xN = xNorm(:);
```

## Appendix 4

### 4. PROGRAM 4 OPTIMUM TIME LAG SELECTION

```
% Program to find optimum time lag
% N1 through N2 are datasets of interest
N1 = 120;
N2 = 122;
k=1;
k1= 1;
for l = N1:N2
    x2 = data{l}{1};
    xmean = mean(x2);
    %
    % Filter section
    sampling_freq = 1000;
    nyq_freq = sampling_freq/2;
    fc = 120;
    wn = fc/nyq_freq;
    [b,a] = butter(16,wn);
    y1 = filtfilt(b,a,x2);
    %
    %Normalization section
    ymean = mean(y1);
    ynorm = y1-ymean;
    x1 = ynorm;
    %
    %
    % Time lag calculation
    n1 =5; %starting value of time lag
    nstep = 5;
    n2 = 440; %end value of time lag
    for n=n1:nstep:n2
        xm = mean(x1);
        x = (x1-xm);
        N = 4000; %window size
        sf_out1 = st_structure_fcn(x, N, n);
        sfn_1(:,k) = sf_out1;
        sfn_1M(k) = (mean(sf_out1));
        k=k+1;
    end
    k=1;
    sf_lag(:,k1) = sfn_1M;
    k1 =k1+1;
end
```



## Appendix 5

### 5. PROGRAM 5 OPTIMUM TIME LAG VS. SF PLOT

```
%plot of time lag
n = n1:nstep:n2;
l=N1:1:N2;

for i =1:(length(l))

    pp1=plot(n,sf_lag(:,i));
    hold on
    grid on
end

%title('Third Order Structure Function vs. Time Lag','fontsize',16);
title('Second Order Structure Function vs. Time Lag','fontsize',16);
ylabel('Average Structure Function [ $\psi^2$ '],'fontsize',16);
xlabel('Time Lag [n] Samples','fontsize',16);
```

## Appendix 6

### 6. PROGRAM 6 OPTIMUM WINDOW SIZE SELECTION

```
% Optimum selection of window size
% Program to find optimum window size
k=1;
k1= 1;
%User can choose any chaotic dataset to determine optimum window size
N1= 85;%Dataset number 85 selected
N2 =86;%Dataset number 86 selected
for l = 85:1:86
    x2 = data{1}{1};
    xmean = mean(x2);
    sampling_freq = 1000;
    nyq_freq = sampling_freq/2;
    fc = 120;
    wn = fc/nyq_freq;
    [b,a] = butter(16,wn);
    y1 = filtfilt(b,a,x2);
    ymean = mean(y1);
    ynorm = y1-ymean;
    x1 = ynorm;

    for N=[200:200:1000 1200 1500 1600 2000 2400 2500....
        3000 4000 4800 5000 6000 8000 10000....
        12000 15000 20000] % window is selected in such a way that it
        %gives whole number of structure function
            xm = mean(x1);
            x = (x1-xm);
            n = 70; %time-lag is fixed to 70

            %Calling structure function
            sf_out1 = fm_structure_fcn1(x, N, n);
            sfn_1M(k) = (mean(sf_out1));
            k=k+1;
        end
        k1=k1+1;
    end
end
```

## Appendix 7

### 7. PROGRAM 7 WINDOW SIZE VS. SF PLOT

```
%  
%Plot of window-size vs. average structure function  
  
n=[200:200:1000 1200 1500 1600 2000 2400 2500 3000 4000 4800 5000 6000 8000  
10000 12000 15000 20000];  
l = N1:1:N2  
  
for i =1:(length(l))  
  
    plot(n,sf_Window_size(:,i),'s-.');  
    hold on  
    legend('chunk 85','chunk 86');  
  
end  
grid on  
  
title('Window size vs. average value of structure function','fontsize',16);  
ylabel('average value of structure function','fontsize',16);  
xlabel('Window Size [samples]','fontsize',16);
```

## Appendix 8

### 8. PROGRAM 8 SF TREND WITH ERROR BAR

```

%ErrorBarPlotFunction
function [dd,i1,Xmean_sf,Xerr_sf,Xstd_sf] =
stErrorBarSf(N1,N2,Ns,Window_of_sf,lag,sf_out)
%
%N1 = initial dataset number
%N2 = final dataset number
%Ns = 120000/(N2-N1+1)

x1 =sf_out;

NN = length(x1);% Number of structure function from dataset N1 to N2
%dummy variables
cc =1;
kk=1;
ll=1;
%
%
mm = fix(NN/Ns)
Sf_mean= zeros(1,mm);
for i1=Ns:Ns:NN

    Xm1 = x1(cc:i1);
    Xmean_sf(:,kk) = mean(Xm1);
    Xstd_sf(:,kk) = std(Xm1);
    Xerr_sf(:,kk) = (std(Xm1)./(sqrt(Ns)));
    cc =1+i1;
    kk=kk+1;
    ll=ll+1;
end
i1=Ns:Ns:NN;
errorbar(i1,Xmean_sf,Xerr_sf,'k-');
%xticks(Ns*[1:mm])
cc=0:Ns:NN;
cc = cc(2:end);
dd=N1:1:N2;
%xticklabels({cc})
%xtickangle(90)
%xt = get(gca,'XTick');
set(gca,'XTick',Ns.*[1:mm],'XTickLabel',dd,'fontsize',10);%structur function wrto chunk
%set(gca,'XTick',Ns.*[1:mm],'XTickLabel',cc,'fontsize',10);%structre function wrto time
xtickangle(45)
hold on
plot(i1,Xmean_sf,'bs')

```

```
title(sprintf('Errorbar plot of sample of structure function from data %d to data %d',  
N1,N2),'FontSize',16);  
%title(sprintf('Averaged Structure function for chunk number %d',zz));  
xlabel(sprintf('sample number with window size of Structure Function %d and  
lag=%d',Window_of_sf,lag),'FontSize',16);  
%xlabel('Time[s]');  
xlim([Ns NN])  
  
hold on  
  
ylabel('Error bar of structure function around its sample mean value','FontSize',16);  
  
grid
```